

A MOLECULAR DYNAMICS STUDY OF THE BUCKLING BEHAVIOUR OF GRAPHENE-REINFORCED ALUMINUM NANOCOMPOSITE PLATE

Ashish K. Srivastava^{1*}, Mithilesh K. Dikshit¹, Vimal K. Pathak¹, Lakshya Khurana²

¹Asst. Prof., Mechanical Engineering Department, Manipal University Jaipur, India

²M.Tech. Scholar, Mechanical Engineering Department, Manipal University Jaipur, India

*e-mail: ashishkumar.srivastava@jaipur.manipal.edu

Abstract. In this study, effects of aspect ratio and perforation on the buckling response of graphene nanosheet (GNS)-embedded aluminum (Al) nanocomposite plate are studied using molecular dynamics (MD) simulations. The periodic system of GS-Al nanocomposite plate is built and simulated using molecular dynamics (MD) based software LAMMPS (Large-scale Atomic/Molecular Massively Parallel Simulator). Embedded atom method (EAM) and Adaptive Intermolecular Reactive Empirical Bond Order (AIREBO) potentials are employed to model the interactions between the atoms of Al and carbon atoms, respectively. It is observed that the buckling strength of square GNS-Al nanocomposite plate deteriorates drastically due to perforation and the same is also true for plates of higher aspect ratio.

Keywords: molecular dynamics, nanocomposites, graphene, buckling, plate

1. Introduction

Two-dimensional (2-D) honeycomb lattice structure of sp^2 -hybridized carbon (C) atoms, Graphene nanosheet (GNS) with extraordinary mechanical properties [1] has been theoretically analysed for more than seven decades [2,3]. Though, these nanosheets were observed as the integral part of 3-D materials, but it was assumed that GNSs were unstable with respect to the formation of curved carbon nanostructures such as fullerenes and nanotubes [4]. In 2004, Novoselov et al. [5] reported naturally-occurring GNSs by experimentation and opened a new window of nanoscience for researchers around the world. Stiffness and failure properties of GNSs are found to be approximately the same as that of carbon nanotubes (CNTs) [6]. However, the high aspect ratio, surface area and thermal conductivity and low production cost, GNSs are favoured over CNTs as a nanofiller reinforcing agent. With the reinforcement of only a small percentage (by weight/volume) of GNSs in polymers, the mechanical properties of the resulting nanocomposite enhances substantially [7].

GNSs have higher surface area than CNTs and can interact with the matrix at its both upper and lower surfaces. The 2-D shape of GNS has improved interlocking with the matrix material and demonstrates a larger interfacial region at GNS–matrix interface than CNT–matrix interface, which leads to better mechanical properties of GNS-reinforced nanocomposite material [8,9]. For example, for 3% reinforcement of GS by weight, the tensile strength and elastic modulus of polyethylene (PE) are enhanced by approximately 77% and 87%, respectively. On the other hand, addition of the same weight fraction of CNTs in PE increases the tensile strength and elastic modulus of PE by only 58% and 57%, respectively [10].

http://dx.doi.org/10.18720/MPM.4222019_10

© 2019, Peter the Great St. Petersburg Polytechnic University

© 2019, Institute of Problems of Mechanical Engineering RAS

Compressive mechanical response of carbon (C) nanofillers are analyzed by various researchers experimentally [11], analytically [12] and through numerical experiments including molecular simulations [13–15]. With continuous improvement and development of less empirical force fields, molecular dynamics (MD) simulations are playing a crucial role in studying the mechanical response of nanofillers. Zhang et al. [16] employed the reactive empirical bond order (REBO) force-field along with Lennard-Jones (LJ) potential to define the interaction between C atoms, similarly, Wang [17] utilized the condensed-phased optimized molecular potential for atomistic simulation studies (COMPASS). Buckling failure behavior of defective CNTs have been examined by Hao et al. [18] with Morse potential integrated with LJ potential.

The extraordinary stiffness and failure properties of GNSs and therefore, enhanced mechanical responses of GNS-reinforced nanocomposites further requires the study of widely used plate-like structures along with the GNS-reinforcement [19]. The load carrying capacity of these GNS-nanostructures subjected to in-plane compression/shear or thermal load is a current area of intense study. For example, the post-buckling response of functionally graded (FG) GNS-reinforced nanocomposite plate under to thermal loading was examined by Shen et al. [20]. In 2018, Srivastava & Kumar [21] have studied the post-buckling behavior of GNS-reinforced nanocomposite plate including the effect of interfacial region. Very recently, Yang et al.[22] have looked into the nonlinear in-plane equilibrium, buckling and post-buckling responses of FG-GNS reinforced fixed and pinned arches subjected to central point load. All these studies are majorly focused on continuum mechanics based study of nanocomposite plate. In order to better understand the buckling or post-buckling response of nanocomposite plate, it is necessary to take care of material response at various loading stages. To capture the response of nanomaterial at nano-level, it is important to employ the molecular simulations while studying the buckling and post-buckling response of GNS-reinforced nanocomposite plate.

In the present study, MD simulations are performed to study the non-linear in-plane instability of nanocomposite plate. Widely used, economical and lightweight metal, aluminum (Al), is chosen as matrix material. Adaptive Intermolecular Reactive Empirical Bond Order Potential function (AIREBO) and Embedded atom method (EAM) are employed, respectively, between the C-C and Al-Al atoms to study the effect of bonded and non-bonded interactions. The effects of aspect ratio and perforation on the buckling and post-buckling responses of nanocomposite plate are also highlighted.

2. Atomistic Modeling

In the current study, a square GNS of sides 250 Å is selected as reinforcing nanofiller and Al is taken as matrix material to model a simplified nanocomposite plate. Open source code, Visual Molecular Dynamics (VMD) is utilized to generate the structure of GNS. The data file generated by VMD was utilized along with the face centered structure of Al atoms, generated in LAMMPS (Large-scale Atomic/Molecular Massively Parallel Simulator) input code. The thickness of nanocomposite plate is taken as 15 Å, thus the width to thickness ratio (i.e., w/h) of nanocomposite plate is 16.67 (> 20) and will behave as thick plate.

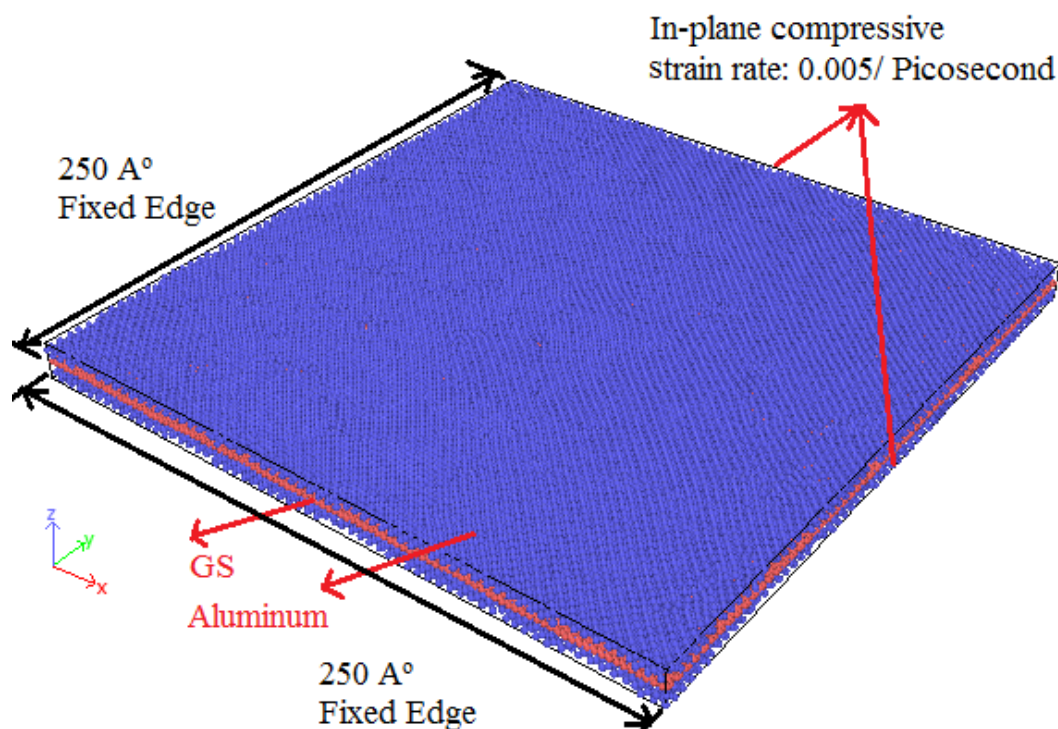


Fig. 1. Simplified GNS-reinforced Al nanocomposite plate subjected to biaxial compressive loading

The interaction potentials that act between the covalently bonded C atoms of GNS are evaluated by AIREBO (Adaptive Intermolecular Reactive Empirical Bond Order) potential function. On the other hand, widely employed Embedded Atom Method (EAM) is utilized to model the pair-wise interactions between Al atoms by EAM/ALLOY potential, which describes the interactions between metals and metal-alloy. The Lennard-Jones (L-J) 12-6 interaction potential (Eq. 1), is also utilized to take care of the non-bonded interactions between GNS and Al matrix material.

$$E = 4\varepsilon \left[\left(\frac{\sigma}{r} \right)^{12} - \left(\frac{\sigma}{r} \right)^6 \right], \quad r < r_c, \quad (1)$$

where, r_c is the L-J cutoff radius, beyond which van-der-Waals (vdW) interaction becomes very weak and therefore neglected. r_c is taken as 2.5σ (i.e. 7.83125 \AA). The potential parameter ε represents the coefficient of well depth energy and σ represents the equilibrium distance between C and Al atoms. The potential parameters for the interactions between C and Al atoms are calculated by widely employed Lorentz-Bertholet (L-B) rule [23]. The potential parameters for individual Al and C atoms are given in Table 1 and thus for interaction zone these are $\sigma = 3.1325 \text{ \AA}$ and $\varepsilon = 0.003457 \text{ eV}$.

Table 1. L-J pair potential parameters for C and Al atoms

L-J Potential parameters	Carbon, C	Aluminum, Al
σ [\AA]	3.41500	2.8500
ε [eV]	0.00239	0.0050

3. Simulation Procedure

After modeling the initial structure of the nanocomposite plate, initially the periodic boundary condition is employed in all the three directions of nanocomposite plate. The potential energy of nanostructure is minimized by conjugate gradient (CG) approach as shown in Fig. 2.

Thereafter, nanostructure was equilibrated by using isothermal–isobaric (i.e., NPT) ensemble at the temperature of 300 K, so that the potential energy and volume of the nanostructure remain relaxed and stable. After the equilibrium process, to observe and analyze the buckling and post-buckling response of nanocomposite plate, the periodic boundary condition in z -direction (i.e., out-of-plane) is replaced with non-periodic shrink-wrapped boundary condition. Therefore, the out-of-plane deformation of nanocomposite plate is accommodated within the system boundary. All edges of the structure are clamped by fixing the forces on them to zero. Thereafter, a constant strain rate of 0.005/picosecond is applied on the x - and y -boundaries of the equilibrated nanostructure.

4. Present Study

Validation. In this section, the MD based approach, utilized to characterize the nanocomposite material and study the buckling and post-buckling response of nanocomposite, is verified with the Rule of mixtures (ROM). An equilibrated dimension of nanocomposite plate is shown in Fig. 2 and corresponding stress-strain diagram in armchair and zigzag direction of GNS is plotted in Fig. 3. The modulus and thickness of interphase zone are taken from literature Srivastava & Kumar [24]. It can be observed from Table 2 that, results are in good comparison with that of analytical solution obtained by ROM.

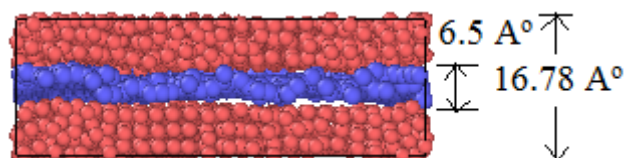


Fig. 2. Equilibrated structure of nanocomposite plate

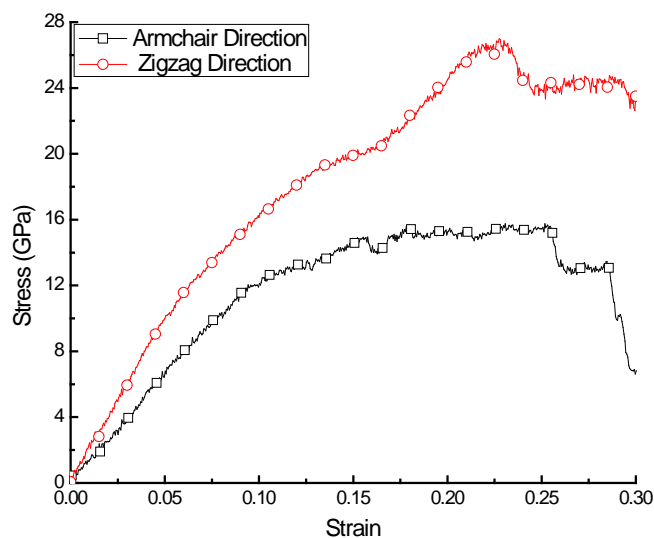


Fig. 3. Stress-strain diagram of nanocomposite material

Table 2. Comparison of Young's modulus for Al -GS aligned nanocomposite

Molecular Dynamics			ROM	% Difference
Armchair	Zigzag	Average		
201.7705	275.6492	238.7099	248.9351	4.1101

Results and Discussion. In this section, initially the post-buckling response of pure Al plate is compared with the results obtained from FEM based software ANSYS. All plates

considered for study are subjected to bi-axial compressive loading and all edges of the plates are clamped. The bi-axial compressive load (N) and the maximum transverse deflection (w_{max}) of the Al plate are normalized as follows

$$\lambda = \frac{Nb^2}{E_m h^3} \quad (\text{with } N = N_x = N_y \text{ for bi-axial loading});$$

$$W^* = \frac{w_{max}}{h}, \quad (2)$$

where E_m represents the elastic modulus of Al matrix material, b and h are the side and thickness of the Al plate.

Thereafter, a separate study is performed to highlight the effect of GNS-reinforcement, aspect ratio and perforation of nanocomposite plate. Since, to analyze the post-buckling response of nanocomposite plate, a constant strain rate is applied in both x - and y -directions, thus the results are also reported in terms of applied strain and W^* (i.e., maximal value of out-of-plane deformation/thickness) of plate.

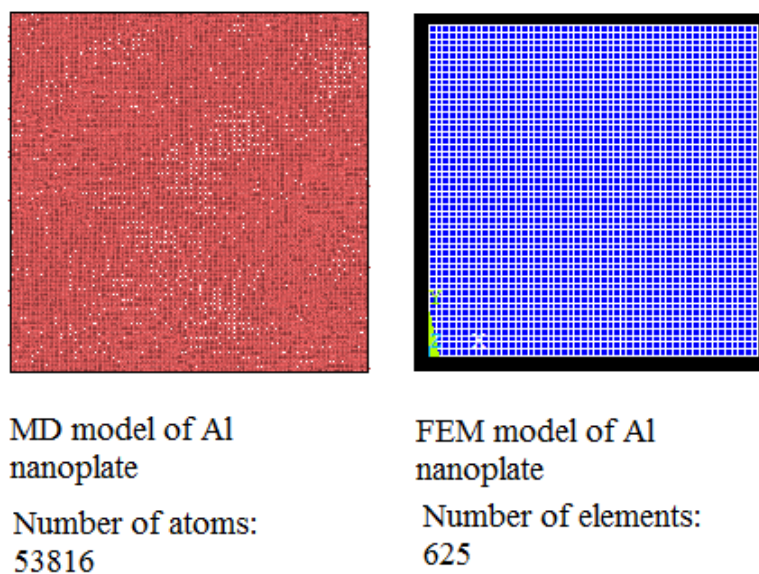


Fig. 4. Comparative diagram between MD and FEM model of plate of same dimension

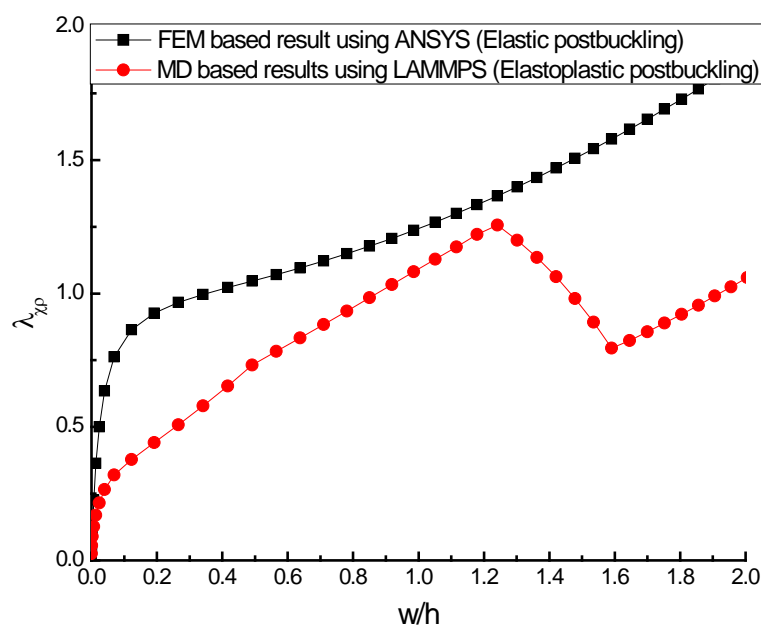


Fig. 5. Comparative post-buckling response of pure Al plate with MD and FEM study

The schematic diagrams of MD and FEM models of nanocomposite plate with number of atoms and elements, respectively, are given in Fig. 4. All edges are taken as clamped in both of the models. The buckling and post-buckling responses of Al plate obtained in both of the methodologies are also given in Fig. 5. It can be observed from Fig. 5 that, using MD, the plate buckles far before than the results reported by the FEM based results. The reason for earlier buckling response is that, in MD simulations, the elastic-plastic behavior of material is taken care whereas, the FEM based study reported in Fig. 5 only considers the elastic response of plate. After, equilibrating the MD model, the plate never remains flat (in contrast to FEM model), and surface irregularity of the plate reduces the buckling strength of the plate, substantially.

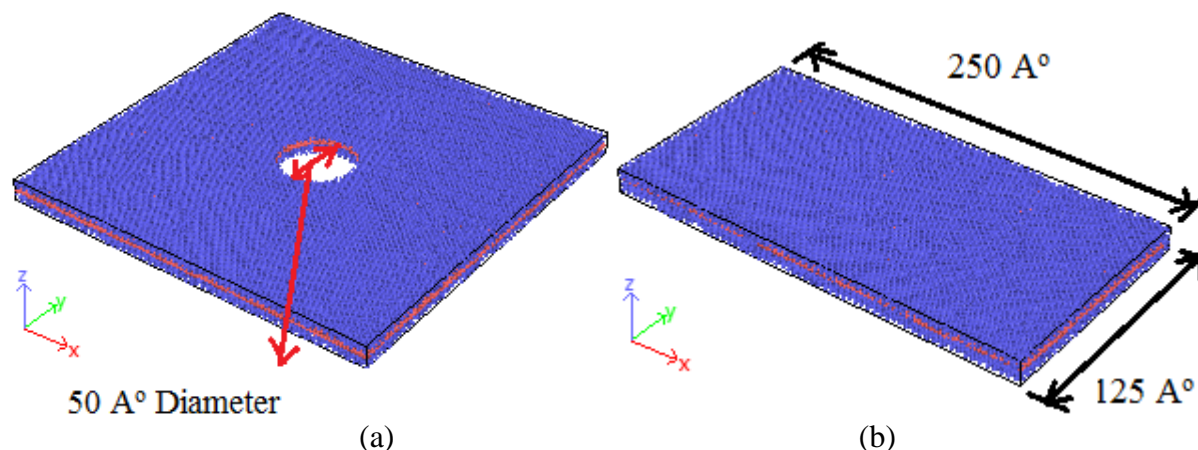


Fig. 6. (a) Perforated GNS-Al nanocomposite plate, (b) GNS-Al nanocomposite plate with aspect ratio ($a/b = 2$)

To visualize the effect of perforation and aspect ratio on the post-buckling response of nanocomposite plate, two different MD models of nanocomposite plate are modeled as shown in Fig. 6. Nanocomposite plate is perforated by a circular hole of 50 Å diameter, and to study the effect of aspect ratio, the width of model is divided by 2.

Figure 7 shows a comparative study between, pure Al plate, GNS-Al nanocomposite plate, effect of perforation and aspect ratio. Results are shown in terms of Strain and normalized out-of-plane deformation of different plates. Buckling strains found from the results are shown in Table 3. It can be observed from Fig. 7 and Table 3, that, GNS-reinforcement enhances the buckling and post-buckling response of nanocomposite plate substantially. Whereas, the higher aspect ratio and perforation have the negative effect on both the buckling load and load carrying capacity of the plate beyond buckling point. By perforating the current plate by a circle of diameter 50 Å, its buckling strength reduces by 36%.

Table 3. Buckling strain for plates considered in the study

S.N.	Type of Plate	Buckling Strain
1	Pure Al	0.001
2	GNS-Al plate	0.03
3	GNS-Al plate with hole	0.019
4	GNS-Al plate having aspect ratio, $a/b = 2$	0.016

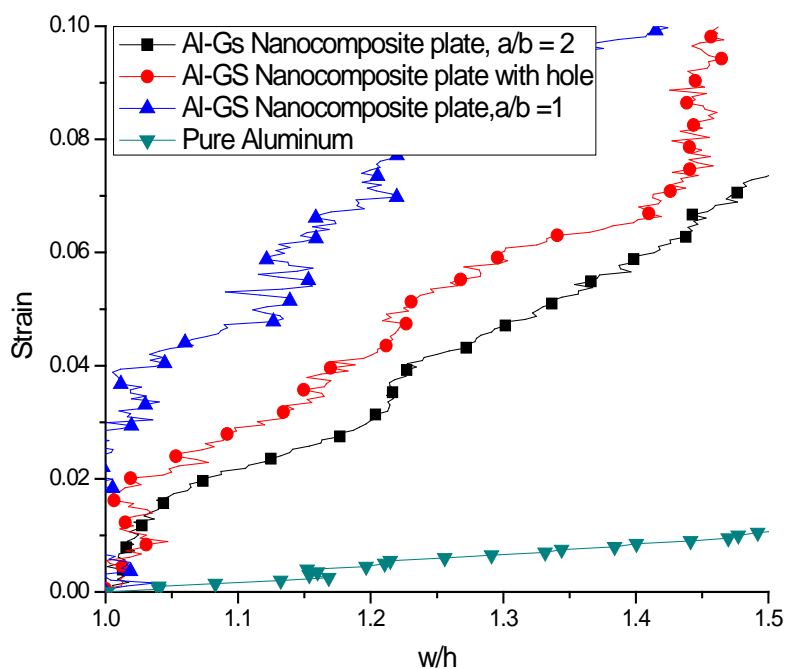


Fig. 7. Post-buckling response of GNS-nanocomposite plate showing the effect of perforation and aspect ratio

5. Concluding Remarks

In the current study, a MD based simulation is performed to study the buckling and post-buckling response of GNS-Al nanocomposite plate. The AIREBO and Embedded Atom Method (EAM) potential are utilized to represent the pair-wise interactions between C and Al atoms, respectively. Bi-axial loading is applied on the nanocomposite plate with the aid of constant strain rate and clamped boundary conditions are enforced on the all edges of plates. Based on the study performed to investigate the effects of GNS-reinforcement, aspect ratio and perforation on the buckling and post-buckling behavior of nanocomposite plate, and the following conclusions are reported:

- GNS-reinforcement in Al matrix leads to substantial increase in the elastic properties of Al matrix material. This enhancement is further substantial in zigzag direction of GNS.
- Enhanced stiffness properties of nanocomposite materials, further enhances the buckling and post-buckling strength of nanocomposite plate.
- The plates having higher aspect ratios demonstrate lesser buckling and post-buckling strength than square plates.
- Perforation reduces the buckling and post-buckling strength of nanocomposite plate.
- It can be established that present approach offers more realistic results than continuum mechanics based studies, due to ability of MD-approach to capture the effect of inherent surface waviness of the plate and to trace the material response at different loading condition at higher geometric scale.

Acknowledgements. The present research work is carried out by utilizing the computation research facilities at the Multiscale Simulation Research Center (MSRC), Manipal University Jaipur (MUJ), India. The authors would like to kindly acknowledge the MSRC, MUJ Jaipur.

References

- [1] Geim AK, Novoselov KS. The rise of graphene. *Nature*. 2007;6: 183–191.
- [2] Wallace PR. The band theory of graphite. *Phys. Rev.* 1947;71(9): 622–634.
- [3] Sharma MP, Johnson LG, McClure JW. Diamagnetism of graphite. *Phys. Lett. A*.

1973;44(7): 445–446.

[4] Fradkin E. Critical behavior of disordered degenerate semiconductors. I. Models, symmetries, and formalism. *Phys. Rev. B*. 1986;33(5): 3257–3262.

[5] Novoselov KS, Geim AK, Morozov SV, Jiang D, Zhang Y, Dubonos SV, Grigorieva IV, Firsov AA. Electric field effect in atomically thin carbon films. *Science*. 2004;306(5696): 666–669.

[6] Ovid'ko I. Mechanical Properties of Graphene. *Rev. Adv. Mater. Sci.* 2013;34(1): 1–11.

[7] Kuilla T, Bhadra S, Yao D, Kim NH, Bose S, Lee JH. Recent advances in graphene based polymer composites. *Prog. Polym. Sci.* 2010;35(11): 1350–1375.

[8] Stankovich S, Dikin DA, Dommett GHB, Kohlhaas KM, Zimney EJ, Stach EA, Piner RD, Nguyen ST, Ruoff RS. Graphene-based composite materials. *Nature*. 2006;442: 282–286.

[9] Kim H, Macosko CW. Processing-property relationships of polycarbonate/graphene composites. *Polymer*. 2009;50(15): 3797–3809.

[10] El Achaby M, Qaiss A. Processing and properties of polyethylene reinforced by graphene nanosheets and carbon nanotubes. *Mater. Des.* 2013;44: 81–89.

[11] Ayatollahi MR, Shadlou S, Shokrieh MM. Multiscale modeling for mechanical properties of carbon nanotube reinforced nanocomposites subjected to different types of loading. *Compos. Struct.* 2011;93(9): 2250–2259.

[12] Li C, Guo W. Continuum mechanics simulation of post-buckling of single-walled nanotubes. *Int. J. Nonlinear Sci. Numer. Simul.* 2003;4(4): 387–393.

[13] Cao G, Chen X. Buckling behavior of single-walled carbon nanotubes and a targeted molecular mechanics approach. *Phys. Rev. B*. 2006;74(16): 165422.

[14] Chang IL, Chiang BC. Mechanical buckling of single-walled carbon nanotubes: Atomistic simulations. *J. Appl. Phys.* 2009;106(11): 114313.

[15] Singh A, Kumar D. Effect of temperature on elastic properties of CNT-polyethylene nanocomposite and its interface using MD simulations. *J. Mol. Model.* 2018;24: 177–178.

[16] Zhang YY, Tan VBC, Wang CM. Effect of strain rate on the buckling behavior of single- and double-walled carbon nanotubes. *Carbon*. 2007;45(3): 514–523.

[17] Wang Q. Buckling of carbon nanotubes wrapped by polyethylene molecules. *Phys. Lett. A*. 2011;375(3): 624–627.

[18] Hao X, Qiang H, Xiaohu Y. Buckling of defective single-walled and double-walled carbon nanotubes under axial compression by molecular dynamics simulation. *Compos. Sci. Technol.* 2008;68(7-8): 1809–1814.

[19] Song M, Kitipornchai S, Yang J. Free and forced vibrations of functionally graded polymer composite plates reinforced with graphene nanoplatelets. *Compos. Struct.* 2017;159: 579–588.

[20] Shen H-S, Xiang Y, Lin F. Buckling and postbuckling of functionally graded graphene-reinforced composite laminated plates in thermal environments. *Compos. Part B*. 2017;119: 67–78.

[21] Srivastava AK, Kumar D. Postbuckling behaviour of graphene-reinforced plate with interfacial effect. *Arch. Mech.* 2018;70(1): 1–34.

[22] Yang Z, Yang J, Liu A, Fu J. Nonlinear in-plane instability of functionally graded multilayer graphene reinforced composite shallow arches. *Compos. Struct.* 2018;204: 301–312.

[23] Boda D, Henderson D. The effects of deviations from Lorentz–Berthelot rules on the properties of a simple mixture. *Mol. Phys. An Int. J. Interface Between Chem Phys.* 2008;106(20): 2367–2370.

[24] Srivastava A, Kumar D. A continuum model to study interphase effects on elastic properties of CNT/GS-nanocomposite. *Mater. Res. Express*. 2017;4(2): 025036.